

# Effect of slot wall jet on combustion process in a 660 MW opposed wall fired pulverized coal boiler

Yong Zhang<sup>\*,1,3</sup>, Yao Fang<sup>1</sup>, Baosheng Jin<sup>1</sup>, Youwei Zhang<sup>2</sup>, Chunlei Zhou<sup>2</sup>, Farooq Sher<sup>3</sup>

<sup>1</sup>Key Laboratory of Energy Thermal Conversion and Control of Ministry of Education, School of Energy and Environment, Southeast University, Nanjing, 210096, China

<sup>2</sup>Jiangsu Frontier Electric Technology Co., Ltd, Nanjing, 211100, China

<sup>3</sup>Department of Chemical and Environmental Engineering, Faculty of Engineering, University of Nottingham, Nottingham NG7 2RD, UK

## Abstract

Numerical investigations of an anti-corrosion design and the combustion process (original conditions and optimal conditions) were conducted for a 660 MW opposed wall fired boiler. In order to solve high-temperature corrosion of the side wall, a scheme is proposed: slotting in the side wall and introducing air (closing-to-wall air) from the secondary air. The effect of anti-corrosion was disclosed in detail by varying the structures of slotting, gas velocities from nozzles and jet inclination angles. The temperature and NO<sub>x</sub> distribution in the furnace at optimized conditions were compared with those at the original operating conditions. Simulation results showed that the structures of the slot and gas velocities from the nozzles have a marked effect on anti-corrosion of the side wall. When the gas velocity was 4 m/s, an inclination angle of the gas velocity was not conducive to anti-corrosion of the side wall. When

---

\*Corresponding author. Tel.: +86-25-83794744; Fax: +86-25-83795508.

E-mail address: [zyong@seu.edu.cn](mailto:zyong@seu.edu.cn) (Y. Zhang). [Farooq.Sher@Coventry.ac.uk](mailto:Farooq.Sher@Coventry.ac.uk) (F. Sher).

21 the gas velocity increases at the middle and bottom of the side wall, the anti-corrosion effect  
22 increases significantly. When the optimal scheme is adopted, the corrosion area of the side wall  
23 decreases obviously, but the furnace temperature and the NO<sub>x</sub> emission increase slightly. The  
24 detailed results of this work promote a full understanding of closing-to-wall air and could help  
25 to reduce the corrosive area in pulverized-coal furnaces or boilers.

26 **Keywords:** Coal combustion, Pulverized coal boiler, High-temperature corrosion, Slotting,  
27 Closing-to-wall air and NO<sub>x</sub> emissions.

## 28 **1 Introduction**

29 At present, China relies on coal to meet 70% of its total energy needs and the coal production  
30 as a major energy resource in China is expected to increase in the near future. However, the  
31 use of a large number of coal-fired resources will exacerbate the air pollution (Mohr and Evans  
32 2009) (Li, Zhuang et al. 2012) (Klein, Andren et al. 1975). As the aggravation of environment,  
33 the standard of NO<sub>x</sub> emission is becoming more and more rigorous. The government and  
34 organizations responsible for environmental protection have established stringent regulations  
35 and legislation for controlling NO<sub>x</sub> emissions from pulverized-coal furnaces (Zhou, Yang et al.  
36 2014). The available methods of reducing the NO<sub>x</sub> emission in pulverized coal boilers are  
37 mainly low-NO<sub>x</sub> combustion technology and tail gas treatment. Selective catalytic reduction  
38 (SCR) (Wang, Zheng et al. 2017) and selective non-catalytic reduction (SNCR) (Qiong, Yuxin  
39 et al. 2013) of the tail gas treatment are very effective methods for controlling the discharged  
40 NO<sub>x</sub>, but these methods are costly and uneconomical. The suitable low NO<sub>x</sub> combustion

41 technology could frequently control NO<sub>x</sub> emissions more economically (Ti, Chen et al. 2016),  
42 however, the application of low NO<sub>x</sub> combustion technology causes high-temperature  
43 corrosion issues in the furnaces and boilers (Zhang 2011) (Liang, Lei et al. 2009).

44 At present, water wall tube's high-temperature corrosion is increasingly prominent in large-  
45 scale utility boilers, which has seriously affected the safe and economic operation of the boilers.  
46 According to a statistics, high-temperature corrosion has been found in more than 80% large-  
47 scale power plant boilers in China and resulted in enormous loss (Xiu-Qing and Zeng 2001)  
48 (Zhou, Pei et al. 2015) (Jiang, Liu et al. 2014). Therefore, it is one of the most urgent problems  
49 to be resolved in the field of heat and power generation to reduce the corrosion and NO<sub>x</sub>  
50 emission simultaneously. Previous research showed that the near wall reducing atmosphere is  
51 considered to be the important cause of high-temperature corrosion in boilers (Zhou, Pei et al.  
52 2015) (Han, Chun-Mei et al. 2004). There are several methods to resolve the high corrosion of  
53 water wall problem among them: the closing-to-wall air technology is in engineering practice  
54 due to its simple and reliable advantages (Wu, Zhuang et al. 2005). The closing-to-wall air can  
55 increase the local O<sub>2</sub> concentration in the high-temperature corrosion zone. It fundamentally  
56 destroys the reducing atmosphere required for the occurrence of corrosion reactions. The  
57 reduction of reducing atmosphere improves the high-temperature corrosion effectively. When  
58 the O<sub>2</sub> concentration is greater than 2%, it is not producing high-temperature corrosion (Zhou,  
59 Pei et al. 2015). In addition, when the proportion of the air volume rate to the total airflow is  
60 less than 5%, it has a negligible effect on the ignition of pulverized coal and the combustion

61 stability (Zhou, Pei et al. 2015) (Lu, Chen et al. 2015) (Chen, Lu et al. 2015).

62 Many researchers have proposed different methods to solve the problem of high-temperature  
63 corrosion of water wall. (Zhang Zhixiang, Cheng Dingnan et al. 2011) proposed a new type of  
64 wall attachment device for preventing the high-temperature corrosion of the tangentially fired  
65 boiler's water walls. The wall air is ejected along the axial direction of the water wall. The  
66 results revealed that the utility device has the advantages of good effect, obvious reduction in  
67 the amount of the closing-to-wall air and the reduction of the nozzle temperature. (Qiu Jihua,  
68 Liming et al. 1999) attained combustion process of a 300 MW front and rear wall opposed coal-  
69 fired boiler by computer numerical simulation under different working conditions. The results  
70 showed that the temperature drop near the water wall is not obvious with the change in the  
71 position of the closing-to-wall air on the front and rear wall. While on the side wall, the high-  
72 temperature corrosion of water wall can be effectively reduced. During solving a problem of  
73 high temperature corrosion of the water wall of the side wall in a 660 MW front and rear wall  
74 opposed coal-fired boiler. (Chen, Lu et al. 2015) found that it can achieve good effect of oxygen  
75 supplementation in the area around the nozzles along the furnace depth direction by using less  
76 vertical closing-to-wall air. But with the diffusion range of closing-to-wall along the high  
77 direction of the furnace wall is limited, resulting in a considerable part of the high temperature  
78 corrosion area cannot get O<sub>2</sub> supply. (Yang, You et al. 2017) found that the concentration of  
79 CO and H<sub>2</sub>S near the side wall was significantly reduced and the reducing atmosphere on the  
80 side wall was reduced by 40% by the injection of near-wall air.

81 Some researchers have concluded that the closing-to-wall air can improve the anti-corrosion  
82 situation of the furnace, but there is no detailed study on how the closing-to-wall air affects the  
83 combustion behaviour in the furnace from the perspective of jet and mixing. In the present  
84 study, the mixing mechanism of closing-to-wall air entering the furnace is analyzed  
85 emphatically from the jet and mixing perspective. An in-depth analysis is made on how to  
86 improve the corrosion resistance of the furnace by closing-to-wall air. The study provides a  
87 detailed reference for the mechanism of closing-to-wall air to improve the anti-corrosion.  
88 Furthermore, structure arrangements, gas velocities from nozzles and jet inclination angles are  
89 simulated under different conditions. The combustion process (original and optimal conditions)  
90 of the furnace is also simulated and analyzed in detail. Previous studies have shown that the  
91 high temperature corrosion is mainly caused by the reducing atmosphere near the side wall,  
92 while the distribution of O<sub>2</sub> concentration is contrary to that of CO and H<sub>2</sub>S. The corrosive area  
93 ratio (the area of O<sub>2</sub> concentration less than 2% accounted for the percentage of total corrosion  
94 area) is an indicator of the effectiveness of the corrosion protection is also discussed. Based on  
95 the analysis of these different conditions, the anti-corrosion performance of the side wall is  
96 explained in depth.

## 97 **2 Materials and experimental methods**

### 98 **2.1 Materials**

99 The coal quality analysis is shown in

101 Table 1. The sulfur content of the coal used in the boiler is very high. Higher the sulfur content  
 102 of the coal used in boiler, the more serious is the boiler corrosion. The value of pulverized coal  
 103 fineness is R90 = 16%. The particle size has a Rosin-Rammer (R-R) distribution (He, Qi et al.  
 104 2015) ranging from 10 to 200  $\mu\text{m}$  with an average particle size of 51.5  $\mu\text{m}$ .

105

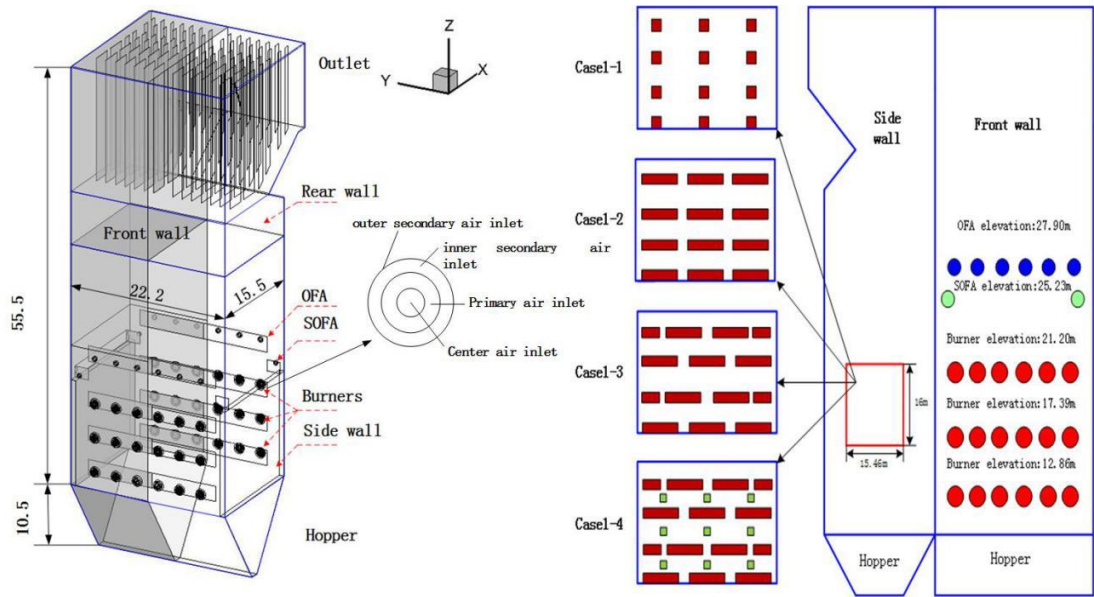
106 **Table 1.** Ultimate and proximate analysis of the coal.

Ultimate analysis					Proximate analysis			Net heating value (MJ/kg)
wt% (as received)					wt% (as received)			
Carbon	Hydrogen	Oxygen	Nitrogen	Surfer	Moisture	Ash	Volatile matter	
47.60	2.84	1.69	0.65	4.51	7.67	35.04	28.70	18.52

107

## 108 2.2 Boiler configurations and operating conditions

109 Fig. 1 shows the schematic configuration of the 660 MW opposed wall fired pulverized coal  
 110 boiler with swirl burners. It is a supercritical once-through boiler. The boiler investigated in  
 111 this study includes a hopper, burner zone, over fire air (OFA), side over fire air (SOFA) and  
 112 outlet. The total height of the boiler is 66 m. The height of the hopper is 10.5 m, while the  
 113 height of the other part of the boiler is 55.5 m. The cross-section of the boiler is a rectangle  
 114 with a width of 22.2 m and a depth is 15.5 m. The boiler adopts the rich/lean burner and the  
 115 distribution of the burner is divided into primary air, secondary air and central air, of which  
 116 secondary air is a swirling flow.



117

118 **Fig. 1.** The schematic configurations of 660 MW pulverized coal boiler along with the  
 119 arrangements for slotting on the side wall.

120 There are 36 burners in total, 18 burners at the front wall, while the other 18 burners at the rear  
 121 wall. The burner nozzles' distribution is at three levels of the furnace height. Under the  
 122 operation of design conditions, only 30 burners are put into use. The burners at the top of the  
 123 rear wall are out of service. Four SOFA nozzles are located above the burner zone. The top  
 124 nozzles of the furnace are OFA ports. The original operating conditions of 660 MWe pulverized  
 125 coal boiler at the power plant are given in Table 2.

126

127

128

129

130

**Table 2.** The original operation data of 660 MWe pulverized coal boiler.

Electrical power block (MWe)	660
Total coal feed rate (kg/s)	85.62
Primary air velocity (m/s)	18.93
Primary air temperature (K)	368
Center air velocity (m/s)	15.20
Center air temperature (K)	573
Inner secondary air velocity (m/s)	8.60
Outer secondary air velocity (m/s)	5.61
Secondary air temperature (K)	573
OFA velocity (m/s)	54.80
OFA temperature (K)	573
SOFA velocity (m/s)	56.87
SOFA temperature (K)	573
Total ratio of OFA and SOFA (%)	25

131

132 The closing-to-wall air comes from OFA and SOFA, and the proportion of the closing-to-wall  
133 air is controlled below 5% of the total air volume. After the initial trial calculations, it is  
134 determined that the numbers of layers of the slots are mainly four and finally the optimization  
135 is carried out on the base of the four layers. Fig. 1 also represents the arrangements of slotting  
136 on the side wall. In simulation, the data on the side wall is taken from a plane 150 mm away  
137 from the side wall and the plane was defined as the near side wall plane. Overall, there are four  
138 different structures. The slot of each working condition is evenly arranged and four cases with

139 different arrangements are first numerically studied, then the optimal condition is chosen from  
 140 these four structures to study the anticorrosion under different operating conditions. The  
 141 required slotting area is determined according to the size of the corrosion zone, the calculated  
 142 parameters with different structures and slot arrangements are given in Table 3.

143 **Table 3.** The calculated parameters with different structures and slot arrangements.

Structure parameters	Case 1-1	Case 1-2	Case 1-3	Case 1-4
L (mm)	670	4500	4500/2500	4500/2500
H (mm)	670	100	100	80
W (mm)	4430	600	600/300	600/300
S (mm)	3330	3900	3900	1810
D (mm)	2293	378	378	378
N	4	4	4	8

144

145 Where L and H represent the length and height of each slot respectively. W represents the  
 146 horizontal distance between two slots. S represents the distance between the two slots in the  
 147 vertical direction. D stands for the horizontal distance between the outermost slot and the wall.  
 148 N represents layers of slots. If the volume of closing-to-wall air is not exceeding 5% of the  
 149 total air volume, it will not have a bad effect on the burning of pulverized coal and the steady  
 150 combustion in the boiler (Chen, Lu et al. 2015). Therefore, the volume of closing-to-wall air  
 151 should not exceed 5% under different conditions of gas velocity from nozzles. Based on the  
 152 above consideration, the side wall closing-to-wall air is chosen and four kinds of working

153 conditions are simulated. The specific calculated parameters with different gas velocities are  
 154 given in Table 4.

155

156 **Table 4.** Calculated parameters with different gas velocities.

Parameters	Case 2-1	Case 2-2	Case 2-3	Case 2-4	Case 2-5
Velocity (m/s)	1	2	3	4	5
Jet flux ratio (%)	1.00	2.10	3.13	4.18	5.22
Air temperature (K)	573	573	573	573	573

157

158 (Min, Li et al. 2014) investigated the effect of over fire air angles on flow characteristics within  
 159 a small-scale model. The results show that an optimal setting of 40° was found for the OFA  
 160 angle. Considering an effect of the angle of the gas jet on the mixing, five different operating  
 161 conditions ranging from 0° to 80° are studied. The specific calculated parameters with  
 162 different jet inclination angle are presented in Table 5.

163 **Table 5.** Calculated parameters with the different jet inclination angles.

Parameters	Case 3-1	Case 3-2	Case 3-3	Case 3-4	Case 3-5
Jet inclination angle (°)	0	20	40	60	80
Velocity (m/s)	4	4	4	4	4

164

165 Based on the results of gas velocity and inclination angle conditions, three different

166 combinations are studied and finally, an optimal condition is obtained. The specific  
 167 combinations of calculated parameters with different gas velocities and inclination angles are  
 168 given in Table 6. The setting of original boundary conditions is listed in Table 2 according to  
 169 the actual operation data of the boiler. The gas velocity of the side wall nozzle is determined  
 170 according to the simulated working conditions in tables. The turbulence specification method  
 171 is intensity and hydraulic diameter.

172 **Table 6.** The combinations of calculated parameters with different gas velocities and  
 173 inclination angles.

Parameters	Case A	Case B	Case C	Arrangements
	6	6	6 /30°	1
	6	6	6	2
Velocity (m/s)	5	5 /6	5 /6	3
	5	4 /5.5	4 /5.5	4
	2 /1	2 /1	2 /1	Square nozzles
Air volume rate (%)	4.9	4.9	4.9	

174

### 175 **2.3 Description of numerical models**

176 The numerical simulations are conducted on the basis of a computational fluid dynamics (CFD)  
 177 coding. According to specific characteristics of the front and rear walls of the coal-fired boiler,  
 178 a three-dimensional mathematical model is established to simulate the combustion process in  
 179 the boiler. The area calculations of the boiler include ash hopper, furnace (Including swirling  
 180 burner, OFA, SOFA) and tail flue. The simulation of swirling burner is performed by separate

181 calculations due to its complex structure. After the flow field calculations, the results of  
182 swirling burner are taken as boundary conditions of the combustion process. Due to complex  
183 structural characteristics and flow symmetry of the boiler and in order to divide the grid more  
184 precisely half of the pulverized boiler structure was selected as the numerical simulation object.  
185 The method of drawing mesh in different domains is used to reduce the pseudo diffusion. It  
186 specifically shows that proper encryption of the mesh in the swirl burner and furnace burner  
187 region. After meshing, the independence of the grid is analyzed, and the total number of grids  
188 in the coal-fired boiler is about 4 million.

189 The combustion in pulverized coal boiler is a complex physical and chemical process involving  
190 chemical reactions, multiphase flows, heat and mass transfer operations. The corresponding  
191 governing equations of CFD are continuity equation, momentum conservation equation and  
192 energy conservation equation. Based on the computational fluid dynamics platform and using  
193 gas-solid two-phase flow model (Euler-Lagrange method) (A. Kohli and D. G. Bogard 1997)  
194 (Belosevic, Srdjan et al. 2012), the flow field of the entire boiler is numerically calculated. The  
195 combustion and heat transfer process in the furnace is numerically calculated using combustion  
196 heat transfer module of the fluent. Realizable K- epsilon model (Zhou, Mo et al. 2011) is used  
197 to simulate the turbulence in the boiler, it can accurately predict the diffusion of circular jet-  
198 flow, rotational flow and secondary flow. For the combustion of the gas phase, non-premixed  
199 combustion model is used because this model allows the prediction of intermediate component,  
200 dissolving effect and rigorous turbulence chemical coupling.

201 For solid phase, the movement of pulverized coal particles in the furnace is a gas-solid two-  
202 phase flow with a chemical in a turbulent flow. The volume fraction of pulverized coal particles  
203 is very small (<10%) relative to the continuous phase, hence, discrete phase model is used to  
204 calculate the motion of particles. The coal particles are considered as discrete particles, which  
205 track the trajectories of pulverized coal particles and calculates the heat and mass transfer  
206 caused by pulverized coal. The process of pulverized coal combustion can be defined as the  
207 precipitation of volatiles and the combustion of coke. Both of the processes are carried out at  
208 the same time and could affect each other. Dual-competitive reaction model is used to simulate  
209 the precipitation of pulverized coal volatiles in this study.

210 The burning of coke is a complex process. It is assumed that the reaction rate of coke is affected  
211 by the rate of oxygen diffusion to the surface of coke and the reaction rate of coke surface at  
212 the same time. Therefore, the kinetic/ diffusion control rate response model is adopted. Because  
213 of the high temperature in the furnace, radiation heat transfer is also considered. The p-1 model  
214 (Hu, Liu et al. 2013) was taken as it is relatively simple and widely used in the radiation heat  
215 transfer in the furnace. In the simulation, the velocity inlet and pressure outlet are taken as  
216 boundary conditions. Overall three-dimensional steady state calculations are adopted. The  
217 standard wall function is used to deal with the near wall turbulent flow in swirl combustion,  
218 the finite-difference methods are used to solve the differential equations, the simple algorithm  
219 and the first-order upwind format are used to solve the governing equations (Hu, Liu et al.  
220 2013). The post-processing method is used for the prediction of NO<sub>x</sub> concentration, and later

221 on, the generation law of nitrogen oxides is applied. A CFD work is completed in three stages:  
222 pre-processing, solver and post-processing. The gambit is used in pre-processing. The fluent  
223 6.3.26 is applied to solve all conservation equations. The numerical solution post-processing is  
224 gathered with the tecplot 360 2010 and origin 2015. Every condition requires an iteration of  
225 30000 steps to converge.

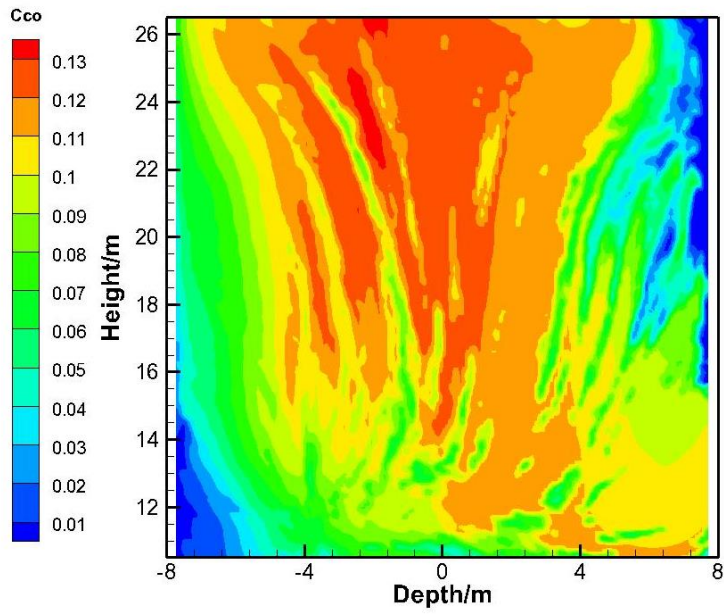
### 226 **3 Results and discussion**

#### 227 **3.1 Validation of the model**

228 To validate the methodologies used in this study, the CFD simulation results are compared with  
229 experimental data of actual operation (Lu, Chen et al. 2015). The boiler modelling, meshing  
230 and model selection is based on the actual situation. Therefore, if the simulation and calculation  
231 methods are correct, the simulation results should be consistent with the experimental data of  
232 actual operation. The comparison of results is listed in Table 7.

233 **Table 7.** Comparison of average parameters of furnace outlet temperature and O<sub>2</sub> concentration  
234 (Lu, Chen et al. 2015).

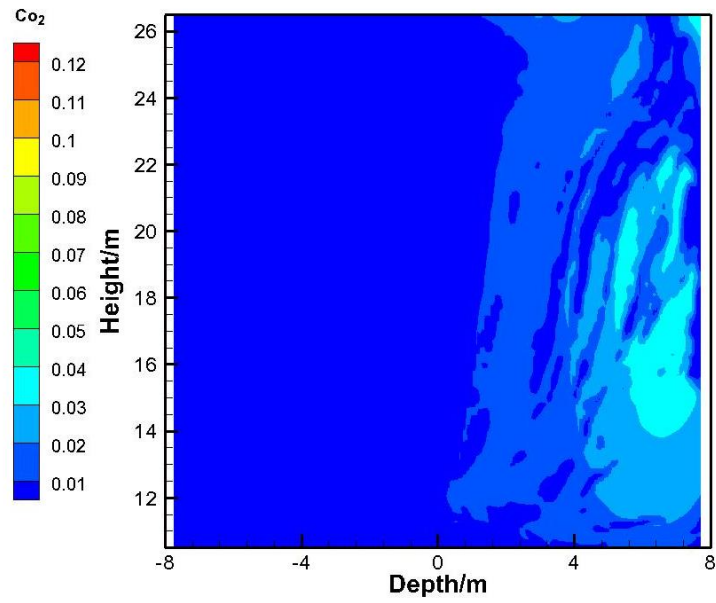
Parameters	Predictions	Original condition	Relative errors
Furnace outlet temperature (K)	1358	1317	3.11%
Furnace O <sub>2</sub> concentration (%)	2.55	3.00	15.00%



235

236

(a) CO concentration distribution



237

238

(b) O<sub>2</sub> concentration distribution

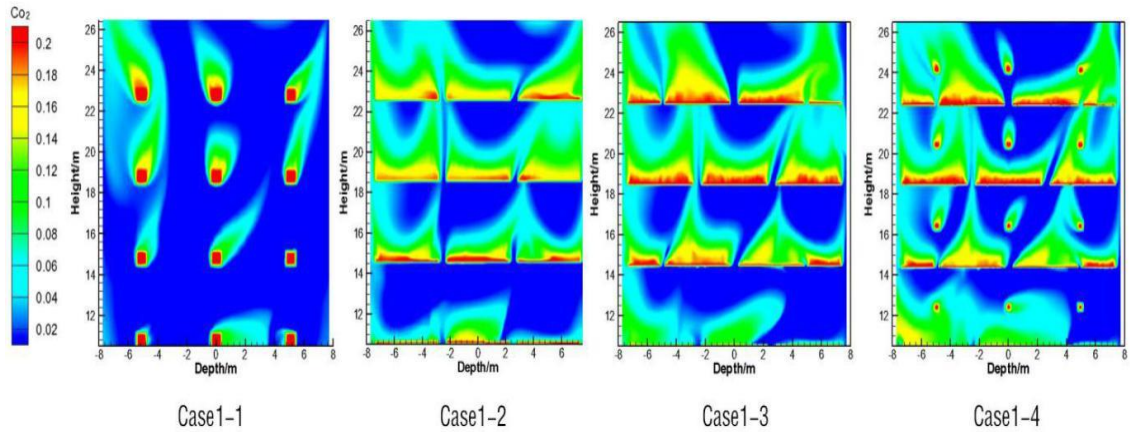
239

**Fig. 2.** O<sub>2</sub> and CO concentration distribution in the near side wall

240 The simulated data shows that the average temperature of the furnace outlet section is 1358 K.  
241 The average concentration (mole fraction) of oxygen in the furnace outlet section is 2.55%, the  
242 actual mean temperature of the furnace outlet is 1317 K and the actual oxygen concentration  
243 in the furnace outlet is 3%. It can be seen that the simulation predictions are very close to the  
244 actual conditions. And the relative errors are comparatively small. Fig. 2 shows the distribution  
245 of CO and O<sub>2</sub> concentration distribution near the side wall. Fig. 2(a) shows a high concentration  
246 of CO near the side wall, whereas the distribution of O<sub>2</sub> is the opposite in Fig. 2(b). It is  
247 consistent with the corrosion area found in boiler shutdown detection. Then it shows that the  
248 simulation methodologies adopted are justified and it can give reliable and accurate predictions  
249 for the 660 MW front and rear wall opposed fired boiler.

### 250 **3.2 Effect of slot structure parameters**

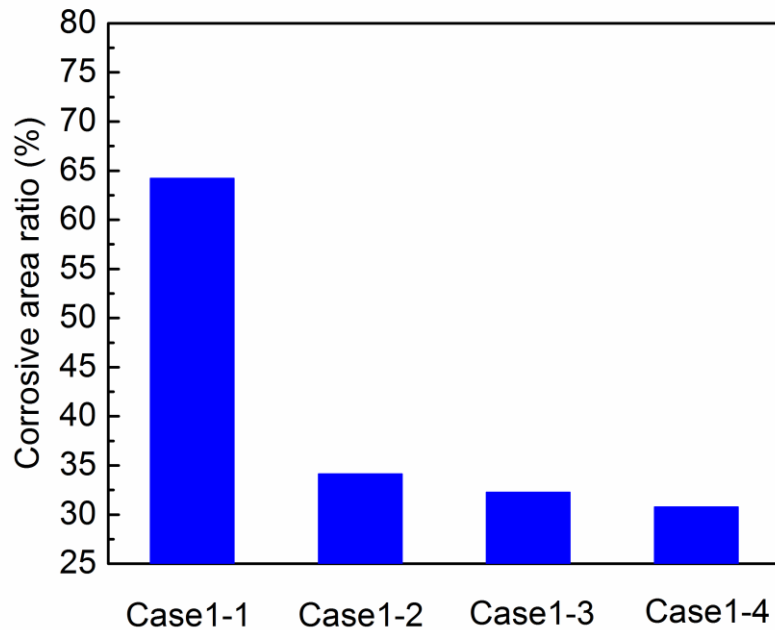
251 Fig. shows the distribution of O<sub>2</sub> concentration in four schemes. It can be clearly seen the  
252 change of O<sub>2</sub> concentration in the near side wall. When the rate of closing-to-wall air is same,  
253 the O<sub>2</sub> coverage area of case1-1 is the smallest, case1-3 and case1-4 are larger than the others.  
254 Comparison of case1-1 and case1-2 in the corrosion zone, the O<sub>2</sub> concentration is relatively  
255 high with the narrow slots. This is because the airflow of the narrow slot has a longer coverage  
256 area when the flow is in the mainstream. So the coverage performance of O<sub>2</sub> with narrow slots  
257 is better than that with square slots in the near side wall.



258

259 **Fig. 3.** The  $O_2$  concentration contour of the different structures and arrangements in the near  
 260 side wall.

261 Fig. shows the corrosive area ratio (the area of  $O_2$  concentration less than 2% accounted for  
 262 the percentage of total corrosion area) of in the near side wall under different conditions. It can  
 263 be clearly seen the changes in the data of the four schemes. In case1-2 and case1-3, the narrow  
 264 slots are divided into two types. As a result, the distribution of  $O_2$  concentration of the latter is  
 265 more uniform than the former. This is due to its staggered arrangement. It makes the gap area  
 266 to get a good airflow cover. Subsequently, a stagger arrangement of slots is better than in  
 267 aligned arrangement.



268

269

**Fig. 4.** The corrosive area ratio of the side wall under different conditions.

270

For case1-4, the mean O<sub>2</sub> concentration increases up to the maximum value, resulting from the

271

closing-to-wall air being injected into the furnace evenly. Comparison of four conditions,

272

arrangement of case1-4 has the best antiseptic effect under the current working conditions. In

273

the latter calculations, slot structures and arrangements are considered as case1-4. Furthermore,

274

the comparison of case1-1 with the others shows that the O<sub>2</sub> coverage in the middle of the

275

corrosion zone is poor than others. Although the overall coverage effect of case1-1 is poor, the

276

coverage of the top of the nozzles is larger than that of other cases. This is because the gas

277

velocity in the middle of the opposed wall firing boiler is larger than the two sides, square slots

278

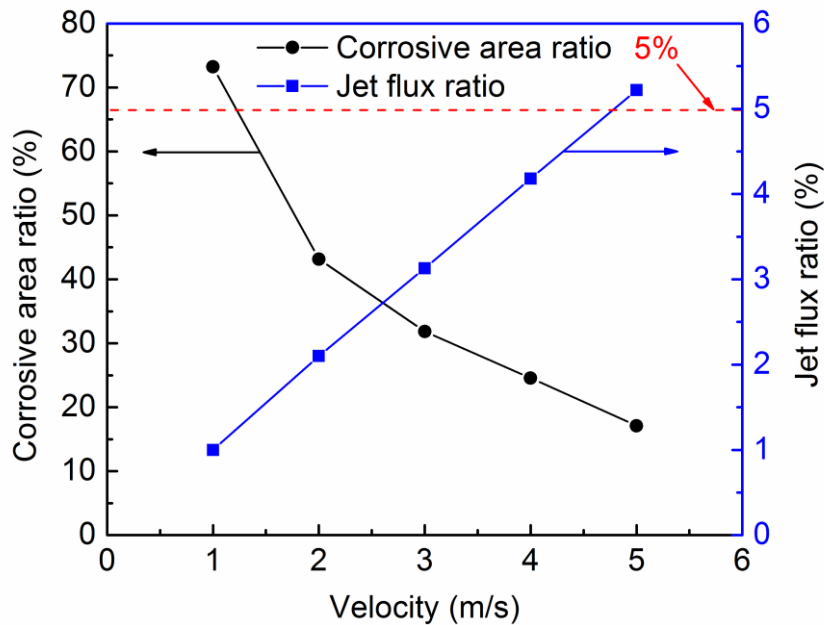
have more gas flow than other cases. Accordingly, there is still more gas in the near wall area

279

when it is mixed with the mainstream.

280 **3.3 Effect of gas velocity from nozzles**

281 The results of corrosive area ratio and the jet flux ratio of pulverized coal boiler are shown in  
282 Fig. . It can be seen that with the increase of velocity, the jet flux ratio of the closing-to-wall  
283 air increases linearly. This is due to the fact that other conditions are constant, while the increase  
284 in velocity is bound to increase the amount of closing-to-wall air, which increases the  
285 proportion of closing-to-wall air in the total air volume.



286

287 **Fig. 5.** The corrosive area ratio and jet flux ratio in different cross-sections with the jet  
288 velocities.

289 On the other hand, the corrosive area ratio on the left shows a downward trend in general. This  
290 can be interpreted as when closing-to-wall air volume increases, relative to the hot flue gas of  
291 the pulverized coal boiler, low-temperature closing-to-wall air reduces the corrosion zone  
292 temperature, and a large amount of air is ejected from the side wall. Therefore, the reductive

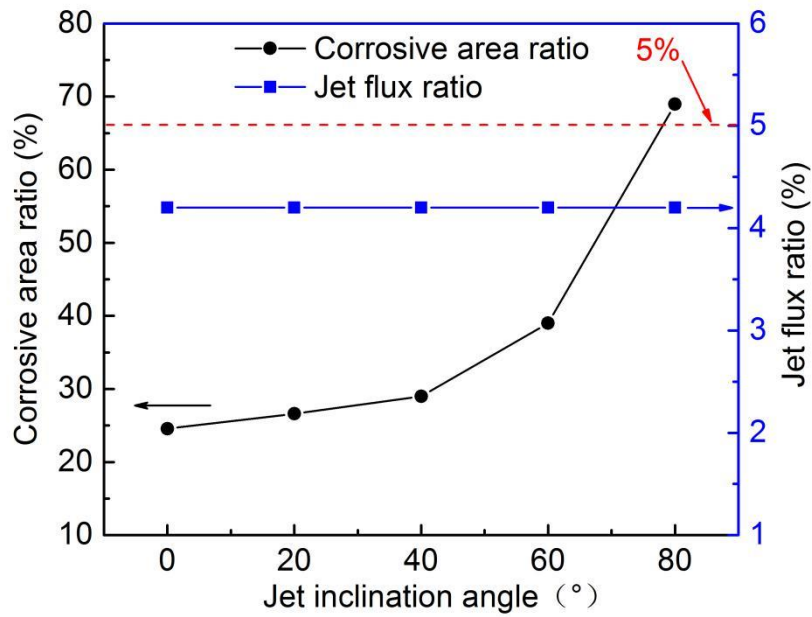
293 atmosphere near the furnace wall can be improved, and this effect is better with the increase of  
294 air flow. When the velocity increases from 1 to 3 m/s, the corrosive area ratio dropped from  
295 73.22 to 31.85%, this reduction of the corrosion area is very clear. When the velocity increases  
296 from 3 to 5 m/s, the corrosive area ratio decreases almost linearly, but the decline is slightly  
297 slower than that in the front. Consequently, it is very effective and important to select the  
298 reasonable gas velocity of closing-to-wall air to reduce the furnace corrosion area. The larger  
299 is the gas velocity, the more air enters means more O<sub>2</sub> it will have to destroy the reducing  
300 atmosphere required for the occurrence of corrosion reactions. The smaller area of corrosion is  
301 caused by reducing atmosphere. However, there are some restrictions on the volume of closing-  
302 to-wall air. When the closing-to-wall air velocity is 5 m/s, the required wall air volume is too  
303 large to exceed the value as seen at the red dotted line in the Fig. . Therefore, it is observed that  
304 the best antiseptic effect can be achieved at the velocity 4 m/s under the current working  
305 conditions.

### 306 **3.4 Effect of jet inclination angle**

307 Fig. shows the variation of O<sub>2</sub> concentration in the near side wall under different injection  
308 angles. Overall, under the condition of 4.18% jet flux ratio, the trend of corrosive area ratio  
309 curve decreases with an increase of jet inclination angle. The results are not the same as the  
310 small hole jet and gas film cooling (Liu 2007) (A. Kohli and D. G. Bogard 1997). For the small  
311 hole jet, when the direction of the jet is perpendicular to the direction of the mainstream, there  
312 is more vigorous interaction and mixing of the jet with flue gas. In this study, the air jet velocity

313 is smaller than the mainstream because of the limitation of the closing-to-wall air volume. The  
314 rigidity of the jet is weaker, and when the closing-to-wall air enters it could be easily diluted  
315 by the flue gas in the furnace which is not very effective for O<sub>2</sub> coverage on the side wall.  
316 However, the jet also has a blocking effect on the mainstream which is effective for O<sub>2</sub> coverage.  
317 Secondly, due to the design and layout of the swirling burner, the flow in the opposed wall  
318 firing boiler furnace is complex, which is different from the general single direction flow.

319 The curve in Fig. indicates that as the jet inclination angle increases, the O<sub>2</sub> coverage rate  
320 becomes lower, it achieves a worse anti-corrosive effect. This is because that the closing-to-  
321 wall air is injected into the furnace from the side wall which has a blocking effect on the  
322 mainstream flue gas coming from the lower part. When the air enters into the furnace vertically,  
323 it has the largest blocking effect on the mainstream near the side wall. Thus, it is difficult for  
324 the mainstream flue gas to reach the side wall, as a result, the reducing atmosphere near the  
325 side wall also reduces. Although the jet flow has a certain angle, the interaction between the  
326 mainstream and the jet flow is enhanced. The jet flow has a greater blocking effect on the  
327 mainstream. So the corrosive area ratio is the least when the jet inclination angle is 0°.



328

329 **Fig. 6.** The corrosive area ratio and jet flux ratio in different cross-sections with the jet  
 330 inclination angle.

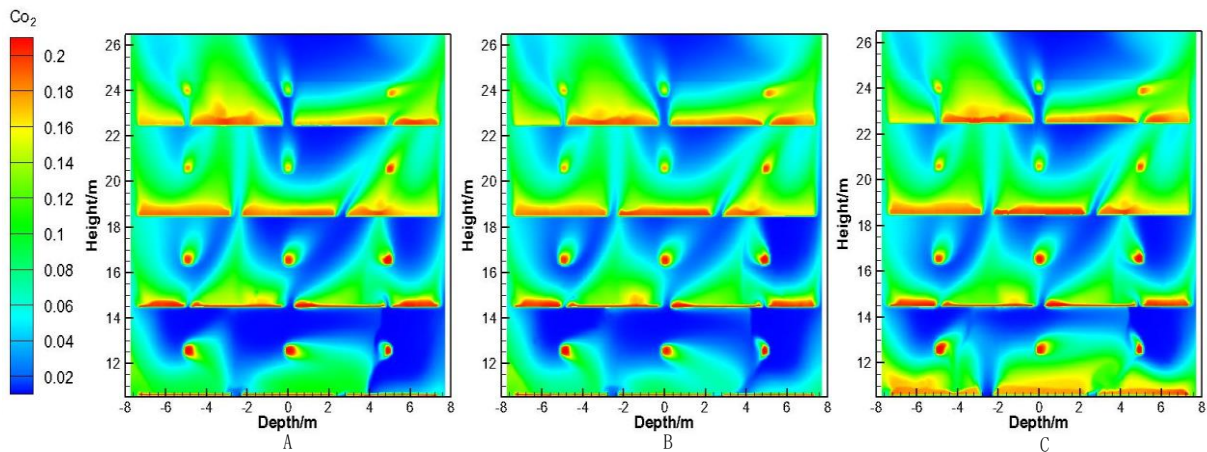
331

332 When jet inclination angle increases, the angle between the jet flow and the mainstream  
 333 becomes smaller. As a result, the ability of the jet flow to block the flow of the mainstream  
 334 becomes weaker. Moreover, when jet inclination angle exceeds  $40^\circ$ , the corrosive area ratio  
 335 increases significantly. As the jet inclination angle reaches  $80^\circ$ , the direction of the closing-  
 336 to-wall air velocity is almost parallel to the direction of the mainstream velocity and the  
 337 corrosive area ratio is almost 70%. At this moment, the jet has the weakest barrier to the  
 338 mainstream. The mixing of the jet and the mainstream is also the weakest. But the blocking  
 339 effect is the main factor in  $O_2$  coverage on the side wall. The reducing atmosphere has not been  
 340 effectively improved, so the corrosive area ratio is the largest.

341

342 **3.5 The optimal strategy**

343 Fig. shows the O<sub>2</sub> concentration contour of three different conditions in the near side wall  
344 when the jet flux ratio is 4.9% (<5%). The O<sub>2</sub> distribution in three cases is almost similar. The  
345 O<sub>2</sub> coverage of the case C is the larger than the others, therefore the reducing atmosphere of  
346 the case C can improve more effectively than other cases. It can be concluded that the  
347 arrangement of the case C is best for anti-corrosion in these three schemes. The difference  
348 among them in O<sub>2</sub> distribution is mainly in the middle and bottom of the side wall.



349 **Fig. 7.** The O<sub>2</sub> concentration contour of three different conditions in the near side wall.  
350

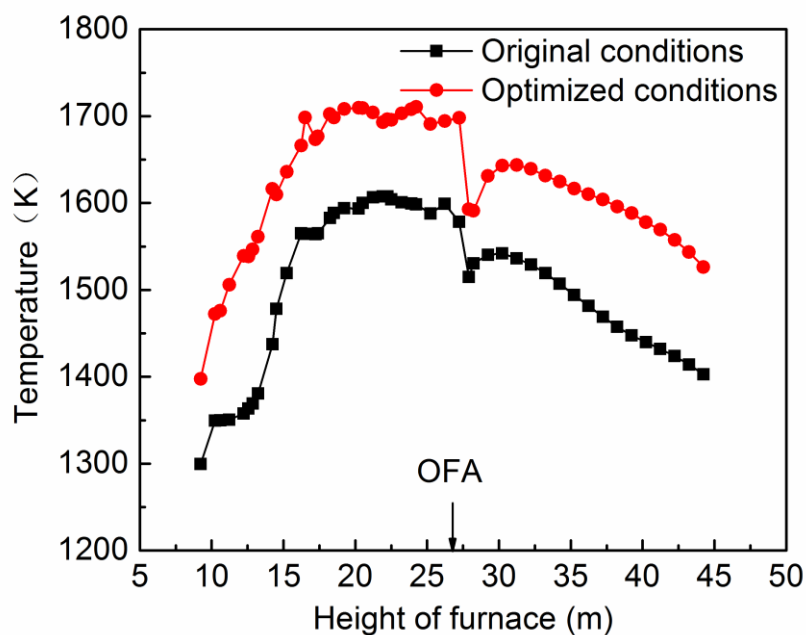
351 The O<sub>2</sub> concentration near to slots is very high. Then it is quickly reduced through dilution  
352 along the furnace height. In a comparison of case A and case B, the O<sub>2</sub> concentration of case B  
353 is slightly higher than that of case A in the middle of the side wall. The cause behind this  
354 phenomenon is mainly due to the relatively large mainstream velocity in the middle of the side  
355 wall. The mainstream velocity in the middle of the side wall is much greater than that on both  
356 sides in the opposed wall firing boiler. The decrease in gas jet velocity at both sides of the wall

357 has a few effects on O<sub>2</sub> coverage. Therefore, with an increase of the gas jet velocity in the  
358 middle of the side wall, the O<sub>2</sub> coverage performance increases significantly. In a comparison  
359 of case B and case C, the most obvious difference is at the bottom of the side wall, O<sub>2</sub> coverage  
360 at the bottom of case C is apparently larger than that of case B. The air jet direction at the  
361 bottom of the side wall of case C has an inclination of 30°. This arrangement is mainly due to  
362 the small amount of flue gas produced at the bottom of the side wall and the smaller mainstream  
363 velocity. After that, the air jet flow easily enters the middle of the furnace and is quickly diluted  
364 with the mainstream. Therefore, when the air jet flow of the lowest layer has a certain angle of  
365 injection, the O<sub>2</sub> concentration of the side wall is greater. The reductive atmosphere is more  
366 effectively improved and anti-corrosion performance is far better. Different positions of the  
367 side wall require a different arrangement of the air jet, for less flue gas at the bottom, it is  
368 necessary to use air jet with a certain inclination angle. This makes the sprayed air more able  
369 to stick to the wall. For a large amount of flue gas and higher velocity in the middle of the side  
370 wall, a larger air jet velocity is required to improve the reducing atmosphere of the side wall.

### 371 **3.6 Effect of the closing-to-wall air on combustion and pollutant emission**

372 Fig. shows the average temperature distribution of flue gas in different cross-sections along  
373 the furnace height. Drawing a comparison between the original conditions and the optimized  
374 conditions, it can be seen that the general trend of the closing-to-wall air's curve is consistent  
375 with the original conditions. At the very start, when the original condition is at the height of 10  
376 meters, the average temperature of the furnace is about 1300 K, while the temperature of

377 closing-to-wall air condition is about 1400 K, with the increase of furnace height, the fuel was  
378 correspondingly increased. The combustion became more and more intense. Therefore, the  
379 temperature keeps going up. When the original condition is at the height of 20 meters, the  
380 average temperature of the furnace is about 1600 K, while the temperature of closing-to-wall  
381 air condition is about 1700 K.



382

383 **Fig. 8.** The average temperature distribution along the furnace height.

384 When the furnace height is higher than the top burner, the fuel quantity is no longer changing,  
385 and the combustion is in a relatively stable period. The temperature of the two conditions  
386 remained relatively stable. However, when it reaches the OFA nozzle, the temperature of the  
387 furnace is rapidly decreased due to the introduction of a large amount of OFA. The temperature  
388 of the original conditions is reduced to 1515 K, while the temperature of the optimized  
389 conditions is reduced to 1593 K. With the burning of pulverized coal, the temperature of the

390 furnace increases again. Finally, with the burnout of pulverized coal the temperature decreases  
391 slowly. Due to the introduction of the closing-to-wall air, the furnace temperature increased  
392 about 70K generally in the most zone, however, it can be seen from table 8 that there is no  
393 obvious effect on the burnout rate of furnace outlet.

394

395

**Table 8.** Burned carbon rate at the furnace outlet.

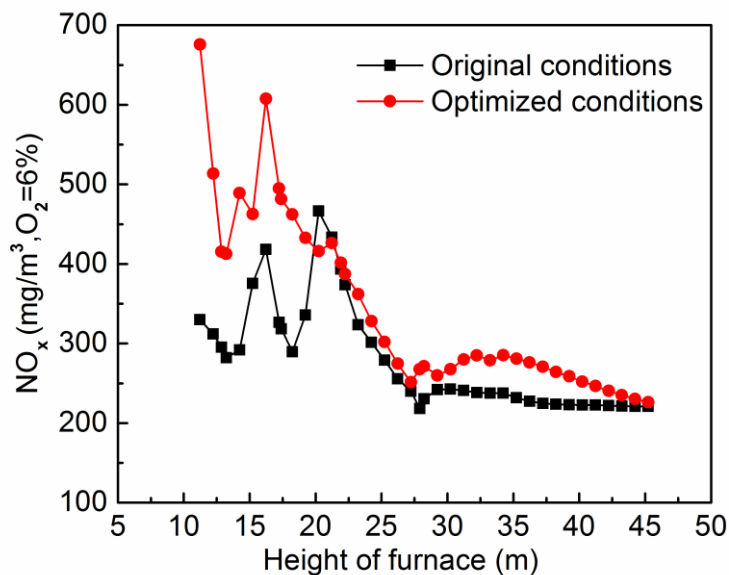
Parameters	Original condition	Optimized condition
Burned carbon rate (%)	99.40	99.38

396

397 The temperature in the original case is lower than the optimum temperature in the furnace. This  
398 is due to the introduction of the closing-to-wall air that has two effects. One is due to the  
399 introduction of cold air which has the effect of reducing the temperature of the furnace flue gas  
400 and the other is the introduction of air which provides a large amount of oxygen, causes the  
401 pulverized coal to further burn and release heat. The heat released by combustion is greater  
402 than the heat consumed by the cold air, consequently, the overall temperature of the furnace is  
403 slightly higher than the original conditions (Lu, Chen et al. 2015).

404 Fig. shows the distributions of NO<sub>x</sub> concentration along the height of the furnace. It can be  
405 seen that NO<sub>x</sub> concentration distribution of both of the two cases is almost similar. In between  
406 the burners, the concentration of NO<sub>x</sub> is high because the O<sub>2</sub> concentration is higher than that  
407 in the vicinity of the burner, as a result, the generated NO<sub>x</sub> exist in large quantities without

408 being reduced. These findings agree with those of (Lu, Chen et al. 2015) and (ZhengqiLi,  
 409 LingyanZeng et al. 2011). Furthermore, at the furnace height of 10 meters, the NOx  
 410 concentration of the original conditions is 330 mg/m<sup>3</sup>. Whereas, the NOx concentration of the  
 411 closing-to-wall air conditions is twice as high as that in the original conditions. This is because  
 412 the introduction of closing-to-wall air has increased the oxygen concentration in the fuel area  
 413 so that air classification effect of the original boiler is weakened.



414

415 **Fig. 9.** Distribution of the average NOx concentration along the furnace height.

416 When the furnace height increases to the OFA zone, The NOx concentration of the original  
 417 conditions and optimized conditions increases significantly. However, the NOx concentration  
 418 at the optimized conditions increases to higher levels. This is related to the temperature of the  
 419 furnace. The furnace temperature of the optimized conditions is higher than that of the original  
 420 conditions and the time of fuel burning becomes shorter. Therefore, in a short time, the NOx

421 concentration increase more obviously when closing-to-wall air conditions are applied. But  
422 with the rapid burn out of the fuel, it eventually reaches a stable value. While the burning of  
423 the original conditions have been kept at a slow speed. It can be found that the NOx  
424 concentration in the original conditions is 220 mg/m<sup>3</sup> in the vicinity of the furnace outlet, while  
425 the NOx concentration in the closing-to-wall air conditions is 226 mg/m<sup>3</sup> which is only a little  
426 higher than that in the original conditions. By introducing the closing-to-wall air from the over  
427 fire air on the side wall, the concentration of NOx in the bottom of the furnace increase  
428 dramatically. However, the concentration of NOx is only slightly higher than that in the original  
429 conditions as combustion continues. Therefore, it is also a very effective way to reduce the  
430 corrosion of the furnace without considering the NOx emission.

#### 431 **4 Conclusions**

432 To reduce the high temperature corrosion of water wall of side wall of 660 MW coal fired  
433 boiler in a power plant, the scheme of slotting in the side wall was proposed. A numerical  
434 investigation was performed to clarify the effect of anti-corrosion in detail by varying the  
435 structure of slotting, gas velocity from nozzles and jet inclination angles. Through the  
436 investigation of different working conditions in 660 MW opposed wall firing boiler, the  
437 following conclusions could be drawn:

438 (1) In terms of influences of the structure and the layout, the coverage performance of O<sub>2</sub> with  
439 narrow slots is better than that with square slots in the near side wall. A stagger arrangement

440 of slots is better than in aligned arrangement. The more slots deployed, the better covered effect  
441 of O<sub>2</sub> will be.

442 (2) In the case of constant slot configuration, the velocity of closing-to-wall air has a marked  
443 effect on O<sub>2</sub> coverage in the near side wall. The greater velocity of gas injection, the better  
444 effect of O<sub>2</sub> coverage. Moreover, with the increase of the mainstream velocity, a greater gas jet  
445 velocity will be required correspondingly. The required air volume will increase significantly  
446 and the entrance of heavy cold air will easily affect the combustion process of the furnace.

447 (3) When the gas jet velocity is 6 m/s, the O<sub>2</sub> coverage performance with gas inclination angle  
448 30° is better than that with 0° at the bottom of the side wall. When the gas jet velocity is 4 m/s.  
449 The angle increases with the horizontal direction, the performance of O<sub>2</sub> coverage becomes  
450 worse on the entire side wall.

451 (4) When the air volume ratio is 4.9 %, the optimum scheme can effectively reduce the area of  
452 the corrosion zone. There is no significant change of burned carbon rate at the furnace outlet.  
453 However, owing to the introduction of closing-to-wall air, the temperature of the furnace and  
454 the NO<sub>x</sub> emissions are slightly increased.

## 455 **Acknowledgement**

456 The authors gratefully acknowledge financial support from the National Key Research and  
457 Development Program of China (Grant No. 2018YFB0605102), A Foundation for the Author

458 of National Excellent Doctoral Dissertation of PR China (201440) and the Fundamental  
459 Research Funds for the Central Universities.

460

## 461 **References**

- 462 A. Kohli and D. G. Bogard. 1997. "Adiabatic Effectiveness, Thermal Fields, and Velocity  
463 Fields for Film Cooling With Large Angle Injection." *Journal of Turbomachinery* 119(2): 352-  
464 358.
- 465 Belosevic, Srdjan, Beljanski, Vladimir, Tomanovic, Ivan, Crnomarkovic, Nenad, Tucakovic  
466 and Dragan. 2012. "Numerical Analysis of NO<sub>x</sub> Control by Combustion Modifications in  
467 Pulverized Coal Utility Boiler." *Energy Fuels* 26(1): 425-442.
- 468 Chen, T., Y. Lu, J. Liu, Q. Huang, G. Chen, B. Jin and Z. Yong. 2015. "Numerical Simulation  
469 on the Optimization of Closing-to-wall Air in a 660 MW Front and Rear Wall Opposed Coal-  
470 fired Boiler." *Proceedings of the Csee*.
- 471 Han, K. H., L. U. Chun-Mei, L. I. Guan-Peng and J. Liu. 2004. "Current Situation and  
472 Discussion About Preventive Measure to the High Temperature Corrosion of Water-wall Tubes  
473 in Large Boilers." *Power System Engineering*.
- 474 He, Z., H. Qi, Y. Yao and L. Ruan. 2015. "Inverse estimation of the particle size distribution  
475 using the Fruit Fly Optimization Algorithm." *Applied Thermal Engineering* 88: 306-314.
- 476 Hu, L., Y. Liu, G. Yi, N. Li and D. Che. 2013. "Effects of Air Staging Conditions on the  
477 Combustion and NO<sub>x</sub> Emission Characteristics in a 600 MW Wall Fired Utility Boiler Using  
478 Lean Coal." *Energy & Fuels* 27(10): 5831-5840.
- 479 Jiang, B., F. G. Liu, K. Liu and H. J. Liu. 2014. "Experimental Research on High Temperature  
480 Corrosion Prevention Technology for Water Wall of Opposed Wall Fired Ultra Supercritical  
481 Boiler." *Applied Mechanics & Materials* 654: 69-73.
- 482 Klein, D. H., A. W. Andren, J. A. Carter, J. F. Emery, C. Feldman, W. Fulkerson, W. S. Lyon, J.  
483 C. Ogle and Y. Talmi. 1975. "Pathways of thirty-seven trace elements through coal-fired power  
484 plant." *Environmental Science & Technology* 9(10).
- 485 Li, J., X. Zhuang, X. Querol, O. Font, N. Moreno and J. Zhou. 2012. "Environmental  
486 geochemistry of the feed coals and their combustion by-products from two coal-fired power  
487 plants in Xinjiang Province, Northwest China." *Fuel* 95(95): 446-456.
- 488 Liang, S. H., H. Lei and E. X. Zhang. 2009. "Study on On-line Monitoring Technology for  
489 High Temperature Corrosion of Boilers." *Journal of Power Engineering*.
- 490 Liu, J. 2007. "Experimental Research on Flat Plate Film Cooling Effectiveness at Different  
491 Injection Angles." *Journal of Engineering Thermophysics* 28(3): 409-411.
- 492 Lu, Y., T. Chen, J. Liu, Q. Huang, G. Chen, B. Jin and Z. Yong. 2015. "Influence of closing-to-  
493 wall air on combustion process in 660MW opposed firing boiler." *Journal of Southeast*  
494 *University* 45(1): 85-90.
- 495 Min, K., Z. Li, Z. Ling, X. Jing and Q. Zhu. 2014. "Effect of overfire air angle on flow

496 characteristics within a small-scale model for a deep-air-staging down-fired furnace." *Energy*  
497 *Conversion & Management* 79(79): 367-376.

498 Mohr, S. H. and G. M. Evans. 2009. "Forecasting coal production until 2100." *Fuel* 88(11):  
499 2059-2067.

500 Qiong, L. I., W. U. Yuxin, H. Yang and L. Junfu. 2013. "Simulation and optimization of SNCR  
501 process." *Ciesc Journal*.

502 Qiu Jihua, Liming, Sun Xuexin and Liu Yonggang. 1999. "The Corrosion of Water Wall in Wall  
503 Fired Boiler." *Journal of Huazhong University Ofence & Technology* 27(1): 63-65.

504 Ti, S., Z. Chen, M. Kuang, Z. Li, Q. Zhu, H. Zhang, Z. Wang and G. Xu. 2016. "Numerical  
505 simulation of the combustion characteristics and NO<sub>x</sub> emission of a swirl burner: Influence of  
506 the structure of the burner outlet." *Applied Thermal Engineering* 104: 565-576.

507 Wang, J., K. Zheng, R. Singh, H. Lou, J. Hao, B. Wang and F. Cheng. 2017. "Numerical  
508 simulation and cold experimental research of a low-NO<sub>x</sub> combustion technology for  
509 pulverized low-volatile coal." *Applied Thermal Engineering* 114: 498-510.

510 Wu, Z., Z. N. Zhuang, T. S. Liu, G. U. Jie and H. C. Xia. 2005. "Study on Slagging Problem in  
511 the Furnace of a Tangential Fired Boiler." *Proceedings of the Csee* 25(4): 131-135.

512 Xiu-Qing, X. U. and R. L. Zeng. 2001. "High Temperature Corrosion of Water Wall for  
513 Tangentially Fired Boiler Furnace." *Power System Engineering*.

514 Yang, W., R. You, Z. Wang, H. Zhang, Z. Zhou, J. Zhou, J. Guan and L. Qiu. 2017. "Effects of  
515 Near-Wall Air Application in a Pulverized-Coal 300 MWe Utility Boiler on Combustion and  
516 Corrosive Gases." *Energy & Fuels* 31(9): 10075-10081.

517 Zhang, J. B. 2011. "Research on High-temperature Corrosion of Ultra-supercritical Opposed  
518 Firing Boiler." *Zhejiang Electric Power*.

519 Zhang Zhixiang, Cheng Dingnan, Wang Yungang and Zhao qinxin. 2011. "Structure Design  
520 and Optimizing Simulation of a New Type Closing-to-wall Air Device." *Journal of Chinese*  
521 *Society of Power Engineering* 31(2): 79-84.

522 ZhengqiLi, LingyanZeng, GuangboZhao, JingLi, ShanpingShen and FuchengZhang. 2011.  
523 "Numerical Simulations of Combustion Characteristics and NO<sub>x</sub> Emissions for Two  
524 Configurations of Swirl Coal Burners in a 300 MWe Wall-Fired Boiler." *Numerical Heat*  
525 *Transfer* 60(5): 441-460.

526 Zhou, H., G. Mo, D. Si and K. Cen. 2011. "Numerical Simulation of the NO<sub>x</sub> Emissions in a  
527 1000 MW Tangentially Fired Pulverized-Coal Boiler: Influence of the Multi-group  
528 Arrangement of the Separated over Fire Air." *Energy & Fuels* 25(5): 2004-2012.

529 Zhou, H., Y. Yang, H. Liu and Q. Hang. 2014. "Numerical simulation of the combustion  
530 characteristics of a low NO<sub>x</sub> swirl burner: Influence of the primary air pipe." *Fuel* 130(5): 168-  
531 176.

532 Zhou, Y. G., L. I. Pei, A. O. Xiang and Z. Hong. 2015. "High temperature corrosion inhibition  
533 for opposed firing boiler based on combustion distribution evenness." Journal of Zhejiang  
534 University.

535